

# Study on the effects of cutting mode on heating when external cylindrical grinding of 40Cr steel

Tuan-Linh Nguyen

**Abstract**— Heat occurs during grinding when the grinding wheel is directly in contact with the part. The generated heat is dependent on the cutting mode, cooling mode, material of the workpiece, etc. Heat is the cause of changes in mechanical and physical properties of metals such as surface burning of the workpiece, residual stress, microscopic cracking, or phase change and affecting the surface quality side of the element. This paper uses an experimental method to study the effects of cutting mode parameters, including feed rate ( $S_d$ ), workpiece speed ( $n_w$ ), and cutting depth ( $t$ ) to heat during external cylindrical grinding of 40Cr steel. The rotation speeds of the grinding wheel is kept constant. A laser sensor with a tolerance of  $\pm 2$  °C is used to measure the surface temperature of the workpiece in the contact area of the grinding wheel. Each double stroke conducted temperature measurement once. An empirically constructed mathematical model and has been rated reliable according to Fisher standards that allow heat control to meet surface quality requirements by adjusting the parameters of the cutting mode accordingly.

**Index Terms**— Heat, feed rate, workpiece speed, cutting depth, external cylindrical grinding.

## I. INTRODUCTION

Grinding is a finishing method used to finalize machine parts that require a high level of surface quality and machining accuracy. Grinding is the process of cutting materials, including cutting, scratching, and rubbing with abrasive particles at a very high speed. Therefore, the heat generated in the grinding process is very much. A significant amount of the heat that is generated at the contact between the grinding wheel and the workpiece is transferred to the workpiece. If the heat transferred to the workpiece exceeds the allowable value, the surface of the workpiece will suffer thermal damage. The damage can be demonstrated by a change in embryo color, appearance of residual stress, microscopic cracking, or phase change. Thermal analysis allows the damage to occur during grinding [1]. In the study [2], Stephen Malkin has shown that the chip burning temperature when grinding can range from 500 to 1000 °C depending on the type of grinding wheel and workpiece material. Qinglong An et al. [3] have researched a new technology of heat transfer during Titanium alloy grinding. In the study [4], Changsheng Guo and Stephen Malkin performed energy zoning during grinding with CBN grinding wheel. Walsh D. et al. [5] analyzed the effect of the workpiece shape on the surface temperature during profile grinding. In this study, we propose an empirical research method to analyze the effect of grinding mode parameters on heat during the external cylindrical grinding process.

Tuan-Linh Nguyen, Department of Mechanical Engineering, Hanoi University of Industry, Hanoi City, Vietnam.

## II. MATERIALS AND METHODS

### A. Experimental setup

Due to the nature of the external cylindrical grinding method, it is difficult to measure the temperature in the grinding zone with the contact sensor. Therefore, choosing the non-contact temperature measurement method, the measurement diagram is shown in Figure 1 [6], [7].

### 1) Experimental machine

Manufacturer: MAGNUM CUT, model: MEG - 1120  
The largest diameter of the workpiece: 200 mm  
The maximum length of the workpiece: 500 mm  
Grinding wheel size: 400x50x203 mm<sup>3</sup>  
The rotation speed of the grinding wheel: 2000 rev/min  
The rotation speed of the workpiece: 0 ÷ 650 revs/min  
The movement speed of the machine table: 0,1 ÷ 5 m/min  
Movement of a wheel stand slide each scale:  
- 0,01 mm/each scale  
- 0,0025 mm/scale  
Motor power rating: 4 kW.

### 2) Grinding wheel

The grinding wheel is made from brown corindon abrasive with strong anti-break ability, anti-oxidation, anti-corrosion, high toughness. Select the appropriate fine particle size when grinding alloy steel to achieve a small surface roughness.

Table 1. Specifications of the grinding wheel

Grain	Brown Corindon (A)	
Symbol of the grinding wheel	V1	
chemical compositions (%)	Al <sub>2</sub> O <sub>3</sub>	≥ 95
	TiO <sub>2</sub>	≥ 1.5 và ≤ 3.8
Vicker Hardness (kG/mm <sup>2</sup> )	HV2200-2300	
Grain size	Smooth	
	Symbol: 180, grain size 90 – 63 μm	
Grinding wheel size	400x50x203 mm <sup>3</sup>	

- Grinding wheel dressing: 3-grain diamond repair head has size of 8,5x40 mm2.

- Wheel dresser mode:  $S_d = 0.5$  m/min,  $t = 0.01$  mm.

### 3) The workpiece

Workpieces for grinding are made from 40Cr steel is alloyed steel with chromium used to make parts with small diameters ( $\varnothing 20 \div 40$ ), relatively complex shapes such as gears, stepping shafts, pins, which require relatively high wear resistance. The chemical composition of 40Cr steel is shown in Table 2.

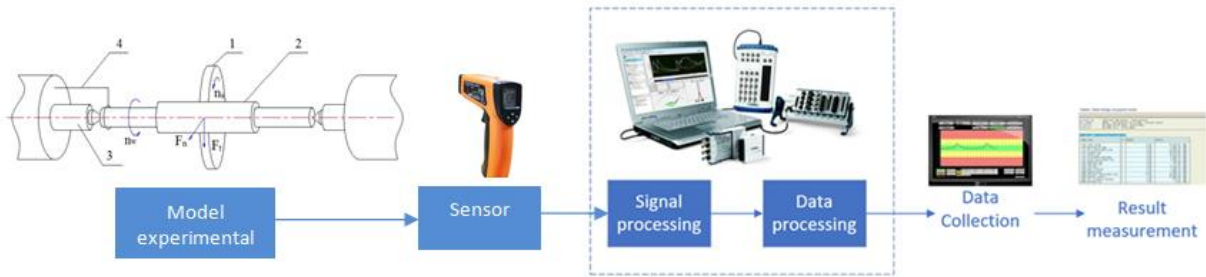


Fig. 1. Thermal measurement diagram on an external cylindrical grinding machine



Fig. 2. Grinding machine MEG – 1120

Table 2. Steel brand used for experiments

Material	Chemical composition (%)
40Cr	C 0.36-0.44, Cr 0.8-1, Mn ≤ 0.8, Si ≤ 0.4, Ni ≤ 0.3

4) Temperature measurement device

Using Taiwan Total Meter DT8016H laser contactless temperature measuring device with a distance ratio of 50: 1 allows accurate temperature measurements at a distance, with a heat source diameter of 1 cm that can be accurately measured at a distance of 50 cm.



Fig. 3. DT8016H laser temperature measuring device

Table 3. Technical specifications of the DT8016H laser temperature measuring device

Technical specifications	Value range
Temperature	-50 °C ~ 1600 °C
Accuracy	± 2 °C
Distance ratio	50:1
Response time & wavelength	500ms & (8-14) um
Resolution	0,1 °C

B. Heat when grinding and workpiece temperature field

1) Heat when grinding

During grinding, heat generated at the contact area between the grinding wheel and the workpiece is transferred to the workpiece, grinding wheel, chip, and coolant. The grinding temperature depends on the heat flow generated in the contact area. The calculation of the grinding temperature is necessary to determine the heat distribution in the grinding zone. The total heat will include [8], [9], [10], [11]:

$$q_t = q_w + q_s + q_{ch} + q_f \quad (1)$$

In which:

$q_w$  is the heat transferred to the workpiece

$q_s$  is the heat transferred to the grinding wheel

$q_{ch}$  is the heat transferred to the chip

$q_f$  is the heat transferred to the coolant

The heat transfers to the workpiece, the grinding wheel and the cooling solution are related to the maximum surface temperature of the  $T_{max}$  workpiece and the liquid burning temperature  $T_b$ . Meanwhile the heat transferred to the chip is related to the average temperature of  $T_{ch}$  chip as follows [12]:

$$q_w = h_w T_{max} \quad (2)$$

$$q_s = h_s T_{max} \quad (3)$$

$$q_f = h_f T_{max} \quad \text{v} \acute{o}i \quad T_{max} \leq T_b \quad (4)$$

$$q_{ch} = h_{ch} T_{ch} \quad (5)$$

In which:  $h_w$ ,  $h_s$ ,  $h_f$ , and  $h_{ch}$  are thermal conductivity coefficients determined by the relationship between heat flow and temperature.

The total heat depends on the grinding power according to the formula:

$$q_t = \frac{P}{bl_c} = e_c \cdot \frac{Q'_w}{l_c} \quad (6)$$

$P$  is the grinding power,  $b$  is the cutting width,  $l_c$  is the contact length,  $e_c$  is the specific grinding energy, and  $Q'_w$  is the specific volume of material removal.

The ratio between workpiece - grinding wheel is:

$$R_{ws} = \frac{q_w}{q_w + q_s} = \frac{h_w}{h_w + h_s} \quad (7)$$

The maximum temperatures reached when grinding with coolant and without coolant is determined as follows:

$$T_{max \text{ wet}} = \frac{q_t - q_{ch}}{\frac{h_w}{R_{ws}} + h_f} \quad (8)$$

$$T_{max \text{ dry}} = \frac{q_t - q_{ch}}{\frac{h_w}{R_{ws}}} \quad (9)$$

2) Temperature field of workpiece during external cylindrical grinding

The temperature field of the workpiece during external cylindrical grinding is the unstable temperature field described by the equation [12]:

$$t = f(r, \tau) \quad (10)$$

The initial workpiece temperature is  $t_0$ , the ambient temperature,  $t_f$ , remains constant.

The temperature field in the symbol is  $\theta = t - t_f$ . For the cylindrical coordinate system, we have differential equations:

$$\frac{\partial \theta}{\partial \tau} = a \left( \frac{\partial^2 \theta}{\partial r^2} + \frac{1}{r} \frac{\partial \theta}{\partial r} \right) \quad (11)$$

With the initial condition  $\tau = 0; \theta_0 = t_0 - t_f$  and the boundary condition:

$$\left( \frac{\partial \theta}{\partial r} \right)_{r=r_0} = -\frac{\alpha}{\lambda} \theta_{r=r_0} \quad (12)$$

The dimensionless residual temperature on the surface of the part is:

$$\frac{\theta_{r=r_0}}{\theta_0} = f(Bi, Fo) \quad (13)$$

In which: Bi is Biot standard:

$$Bi = \frac{\alpha r_0}{\lambda} \quad (14)$$

Fo is Fourier standard:

$$Fo = \frac{a\tau}{r_0^2} \quad (15)$$

The workpiece's thermal conductivity is  $\lambda$ . The coefficient of heat generation from the workpiece surface to the ambient is  $\alpha$

C. Experimental method

We study the thermal and temperature when grinding 40Cr steel with a hardness value of 50 HRC. Change the feed rate to three levels: 0.3, 0.4, 0.5 mm/rev. Workpiece speed is set at three levels: 100, 150, 200 rpm. The cutting depth is also set at 3 levels: 0.005, 0.015, 0.025 mm.

Table 4. Experimental conditions [13]

Parameters	Levels			Variable range
	Above level +1	Base level 0	Lower level -1	
Feed rate $S_d$ , mm/rev	0.5	0.4	0.3	0.1
Rotation speed of the workpiece $n_w$ , rpm	200	150	100	50
Cutting depth $t$ , mm	0.025	0.015	0.005	0.01

Choose a simplified first-order modeling plan, each factor changes by 3 levels. Thus, the number of experiments to be performed is  $N = 2^3 = 8$  experiments [14].

The simplified first-order mathematical model has the form:

$$y = b_0 + b_1x_1 + b_2x_2 + b_3x_3 \quad (16)$$

In which:  $x_1$  is the base e logarithm of the feed rate,  $S_d$

$x_2$  is the base e logarithm of the rotation speed of the workpiece,  $n_w$

$x_3$  is the base e logarithm of the cutting depth,  $t$

$y$  is the base e logarithm of the the maximum temperature  $T$ .

The mathematical model (16) can be written as a matrix as follows:

$$[X] * [B] = [Y] \quad (17)$$

$$[X^T] * [X] * [B] = [X^T] * [Y] \quad (18)$$

Let  $[M] = [X^T] \cdot [X]$ , deduce the solution of the system is:

$$[B] = [M^{-1}] * [X^T] * [Y] \quad (19)$$

Inside:

$$X = \begin{bmatrix} 1 & -1.203 & 4.605 & -5.298 \\ 1 & -0.693 & 4.605 & -5.298 \\ 1 & -1.203 & 5.298 & -5.298 \\ 1 & -0.693 & 5.298 & -5.298 \\ 1 & -1.203 & 4.605 & -3.912 \\ 1 & -0.693 & 4.605 & -3.912 \\ 1 & -1.203 & 5.298 & -3.912 \\ 1 & -0.693 & 5.298 & -3.912 \end{bmatrix}; Y = \begin{bmatrix} 5.617 \\ 5.645 \\ 5.638 \\ 5.670 \\ 5.707 \\ 5.733 \\ 5.720 \\ 5.743 \end{bmatrix}$$

$Y$  is the matrix of  $\ln(T)$  with  $T$  is the maximum temperature measured on the workpiece surface.

Table 5. Planning table of experimental parameters with 40Cr steel

No	Input parameters							T (°C)	Ln( $S_d$ )	Ln( $n_w$ )	Ln( $t$ )	Ln( $T$ )
	Variable encoding				Experimental variables							
	$X_0$	$X_1$	$X_2$	$X_3$	$S_d$ mm/rev	$n_w$ rpm	$t$ mm					
1	+1	-1	-1	-1	0.3	100	0.005	275	-1.203	4.605	-5.298	5.617
2	+1	+1	-1	-1	0.5	100	0.005	283	-0.693	4.605	-5.298	5.645
3	+1	-1	+1	-1	0.3	200	0.005	281	-1.203	5.298	-5.298	5.638
4	+1	+1	+1	-1	0.5	200	0.005	290	-0.693	5.298	-5.298	5.670
5	+1	-1	-1	+1	0.3	100	0.025	301	-1.203	4.605	-3.912	5.707
6	+1	+1	-1	+1	0.5	100	0.025	309	-0.693	4.605	-3.912	5.733
7	+1	-1	+1	+1	0.3	200	0.025	305	-1.203	5.298	-3.912	5.720
8	+1	+1	+1	+1	0.5	200	0.025	312	-0.693	5.298	-3.912	5.743

III. RESULTS AND DISCUSSION

Using MATLAB software to program and calculate the results. We have a mathematical model of the relation between the temperature and the input parameters:

$$y = 5.8881 + 0.0534x_1 + 0.0249x_2 + 0.0601x_3 \quad (20)$$

Or it can be written as an exponential function like this:

$$T = 360.719S_d^{0.0534}n_w^{0.0249}t^{0.0601} \quad (21)$$

To assess the appropriateness of the regression equation is to check whether the model obtained correctly describes our experiments or not.

We use Fisher standard to compare between Fisher calculation ( $F_{cal}$ ) and Fisher according to the table ( $F_{tab}$ ) [14]:

$$F_{cal} < F_{tab}(P, k_1, k_2) \quad (22)$$

In which:

$$k_1 = N - n - 1 \text{ and } k_2 = N(m - 1)$$

N: number of experiments (N = 8)

n: number of factors affecting the test results (n = 3)

m: number of repetitions of the experiment (m = 3)

So:  $k_1 = 4$ ;  $k_2 = 16$

$$F_{cal} = \frac{S_c^2}{S_r^2} \quad (23)$$

Compatible variance:

$$S_c^2 = \frac{m}{N - n - 1} \sum_{i=1}^N (\bar{y}_i - \hat{y}_{tb})^2 \quad (24)$$

Repetitive variance:

$$S_r^2 = \frac{1}{N} \sum_{i=1}^n S_i^2 = \frac{1}{N(m-1)} \sum_{i=1}^N \sum_{j=1}^m (y_{ij} - \bar{y}_i)^2 \quad (25)$$

In which:

$\hat{y}_i$ : Experimental results No. i calculated according to the regression equation

$\bar{y}_i$ : The average value of m times experiments in the i<sup>th</sup> experiment

$y_{ij}$ : the value of the i<sup>th</sup> experiment in the j<sup>th</sup> iteration

$\bar{y}_i - \hat{y}_i$ : Error between theory and experiment in an i<sup>th</sup> experiment.

Basing on experimental results according to Table 5 and the regression (21), we have:

$$S_c^2 = 55.6; S_r^2 = 44$$

According to the Fisher standard [14]:

$$F_{cal} = 1.26 < F_{tab}(4, 16, 0.95) = 3.0$$

Thus, mathematical models (21) are consistent with reality.

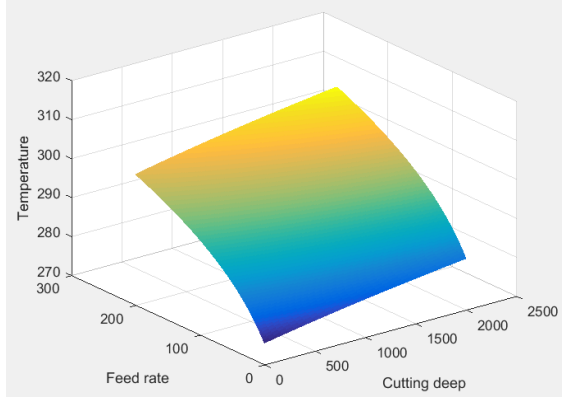


Fig. 4. Graph showing the relationship between temperature and feed rate, cutting deep when nw = 100 rpm

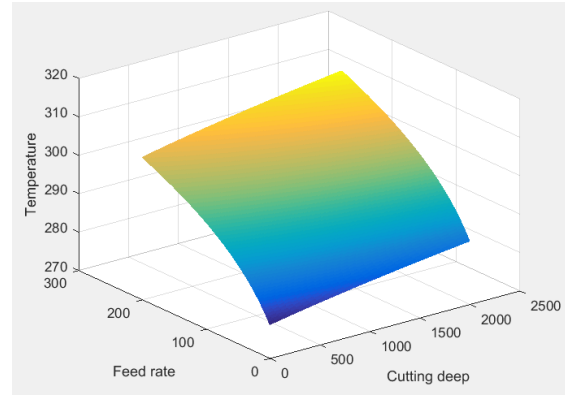


Fig. 5. Graph showing the relationship between temperature and feed rate, cutting deep when nw = 150 rpm

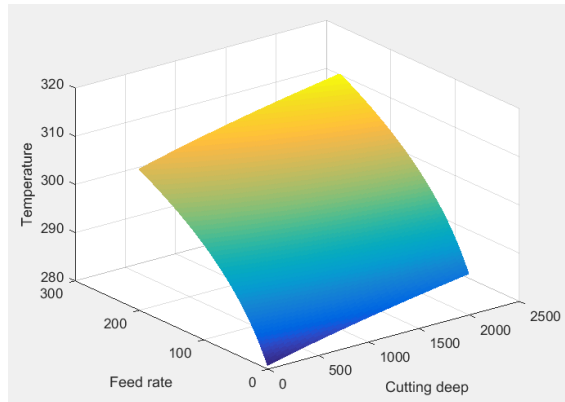


Fig. 6. Graph showing the relationship between temperature and feed rate, cutting deep when nw = 200 rpm

The mathematical model (21) and the graphs in Figures 4, 5, and 6 show that as the feed rate parameters, the workpiece speed, and the cutting depth are increased, the surface temperature increases. The cutting depth has the strongest influence on temperature, then the feed rate and rotation speed of the workpiece have the least influence. Mathematical modeling (21) guarantees 95% confidence, and it fits reality.

IV. CONCLUSION

An experimental model was built with a grinder system measuring equipment to study the effect of cutting mode parameters on the heat generated during the 40Cr steel grinding process on the external cylindrical grinding machine. Using the experimental planning method with three input parameters are feed rate, workpiece speed, and cutting depth, the output parameter is the temperature on the workpiece surface. An exponential mathematical model has been developed with the temperature function dependent on the feed rate variables, workpiece speed, and cutting depth. The temperature depends mostly on the cutting depth, then on the feed rate, and the workpiece speed has the least effect. This mathematical model is also evaluated according to Fisher's standard to ensure reliability.

REFERENCES

[1] Hrala, Michal; Batako, Andre; Morgan, Michael. *Theory and thermal analysis of high efficiency deep grinding process*. Scientific Bulletin Series C: Fascicle Mechanics, Tribology, Machine Manufacturing Technology; Baia Mare Vol. 19, (2005): 1-6.  
 [2] Stephen Malkin. *Grinding Fundamentals and Applications*. Amer Society of Mechanical, 1989.

- [3] Qinglong An, Yucan Fu, Jihua Xu. *New technology on enhancing heat transfer during grinding of titanium alloy*. Industrial Lubrication and Tribology 62(3):168-173. DOI: 10.1108/00368791011034557.
- [4] Changsheng Guo, Stephen Malkin. *Energy partition and cooling during grinding*. Journal of Manufacturing Processes, pg. 151, vol. 2, No. 3, 2000.
- [5] Walsh, D. Torrance, A A. *Influence of form on surface temperatures in form grinding*. Proceedings of the Institution of Mechanical Engineers, pg. 601, 1999.
- [6] Tuan-Linh Nguyen, Nhu-Tung Nguyen, Long Hoang. *A study on the vibrations in the external cylindrical grinding process of the alloy steels*. International Journal of Modern Physics B, vol. 34, 22n24, pp.2040150, 2020, DOI: 10.1142/S0217979220401505.
- [7] Tuan-Linh Nguyen, Van Trong Thai, Long Hoang. *Experimental investigation of the effects of process parameters on cutting force in external cylindrical grinding operation*. Tribology in Industry, Vol. 43, No. 2, 2021/DOI: 10.24874/ti.1013.11.20.01.
- [8] Jin, T; Stephenson, D J. *Analysis of grinding chip temperature and energy partitioning in high-efficiency deep grinding*. Proceedings of the Institution of Mechanical Engineers, pg. 615, 2006. Doi: 10.1243/09544054JEM839.
- [9] O'Donovan, T S; Murray, D B; Torrance, A A. *Jet heat transfer in the vicinity of a rotating grinding wheel*. Proceedings of the Institution of Mechanical Engineers, pg. 837, 2006. Doi: 10.1243/09544062JMES265.
- [10] Jun Yi, Wei Zhou, and Zhaohui Deng. *Experimental Study and Numerical Simulation of the Intermittent Feed High-Speed Grinding of TC4 Titanium Alloy*. MDPI metals, 2019. DOI: 10.3390/met9070802.
- [11] W.B. Rowel, M.N. Morganl, A. Batakol & T. Jin. *Energy and temperature analysis in grinding*. Transactions on Engineering Sciences vol 44, 2003.
- [12] Frank Kreith. *The CRC handbook of thermal engineering*. CRC Press LLC, 2000.
- [13] Tuan-Linh Nguyen, Nhu-Tung Nguyen, Long Hoang. *Multi-objective optimization using the genetic algorithms for the external cylindrical grinding process of 9CrSi alloy*. International Journal of Modern Physics B, vol. 34, 22n24, pp. 2040161, 2020, DOI: 10.1142/S021797922040161X.
- [14] Douglas C. Montgomery. *Design and Analysis of Experiments*, Wiley, 10th edition, 2019.